69.20 ✓

CONF-8909141--10

DETAILED ANALYSIS OF URANIUM SILICIDE DISPERSION FUEL SWELLING*

CONF-8909141--10

DE90 010418

by

Gerard L. Hofman
Argonne National Laboratory
Argonne, Illinois 60439

and

Woo-Seog Ryu
Korea Atomic Energy Agency
(Sponsored by the IAEA)

To be Presented
at the

XI. International Meeting on
Reduced Enrichment for Research and Test Reactors

September 10-13, 1989
Berlin, Federal Republic of Germany

---

*Work supported by the U.S. Department of Energy under Contract No. W-31-109-ENG-38

To be presented at the meeting on Reduced Enrichment
for Research and Test Reactors, Berlin, Sept. (1989)

DETAILED ANALYSIS OF URANIUM SILICIDE DISPERSION FUEL SWELLING

by

Gerard L. Hofman

and

Woo-Seog Ryu*

Argonne National Laboratory
9700 S. Cass Avenue
Argonne, Illinois 60439

ABSTRACT

Swelling of U_3Si and U_3Si_2 is analyzed. The growth of fission gas bubbles appears to be affected by fission rate, fuel loading, and microstructural change taking place in the fuel compounds during irradiation. Several mechanisms are explored to explain the observations. The present work is aimed at a better understanding of the basic swelling phenomenon in order to accurately model irradiation behavior of uranium silicide disperson fuel.

---

* KAERI, Korea, Sponsored by the IAEA.

I. Introduction

Post irradiation data on Uranium Silicide dispersion fuels developed at ANL have been reported at previous RERTR meetings [1,2,3], and various aspects of fuel swelling have been discussed in these publications. More recently we have begun computer modeling of fuel plate irradiation behavior [4]. Successful modeling requires a more fundamental understanding of the fuel swelling phenomenon. This task is pursued by studying the basic irradiation behavior of uranium silicides using charged particle irradiations and experiments with the ANL Intense Pulsed Neutron Source (IPNS). In addition a more detailed analysis of available postirradiation data was undertaken. The initial result of the latter is the subject of the present paper.

II. Postirradiation Examination

Postirradiation examination of the miniplates consists of visual examination, γ-scanning and thickness measurements followed by immersion volume measurements, and optical metallography, scanning electron microscopy (SEM) and burnup determination by isotopic analysis of selected plates.

The average burnup of each plate is calculated by determining the relative γ-activity with respect to at least one plate in each irradiation module on which isotopic burnup measurements are done.

The volume change of each plate ΔV^{PL} is measured after chemically stripping the oxide layer that formed during irradiation. Fuel swelling, ΔV^{F}, is calculated from these immersion volume data with the assumption that, since the cladding density remains unchanged, the volume change is entirely due to swelling the fuel core, ΔV^{C}, with the following relation:

$$\Delta V^F = \frac{\Delta V^C + (\Delta Vo^P - \Delta V^P)}{\Delta Vo^F}$$

where ΔVo^P and ΔV^P are respectively the as-fabricated porosity fraction in the core before and after irradiation, and ΔVo^F is the as-fabricated fuel volume fraction in the core.

Residual as-fabricated porosity is determined by measuring the area fraction on metallographic sections of selected plates. This measurement is facilitated by the fact that the porosity consolidates early during the irradiation as a result of radiation enhanced diffusion as illustrated by core microstructure of depleted uranium silicide shown in Fig. 1. It can be assumed that the depleted "fuel" does not swell to any significant degree. Fuel swelling in the enriched plates will first consume this as-fabricated porosity before plate swelling occurs. The change in as-fabricated porosity as a function of fission density, FD, is shown in Fig. 2. Values of V^P for plates that were not metallograhically examined are determined from Fig. 2 by interpolation.

III. Fuel Swelling

Fuel particle swelling of LEU, MEU and HEU U_3Si_2 and U_3Si as a function of fission density is plotted in Figs. 3 and 4. The swelling is comprised of three major components: (1) a volume change due to the transformation to a higher silicon phase as a result of uranium burnup, (2) volume increase due to the accumulation of non-gaseous fission products, and (3) volume increase due to fission gas accumulation.

The volume change due to uranium burnup was calculated using the most current uranium-silicon equilibrium phase diagram and measured densities of the phases involved. The amounts of non-gaseous fission products were determined with the aid of published fission yield data for ^{235}U. The fission products were grouped according to their chemical behavior vis a vis uranium silicide. These contributions to volume change were estimated by evaluating their solubility in the fuel and the tendency to form compounds with each other and with uranium and silicon. These first two contributions to swelling, i.e., phase transformation and non-gaseous fission products were combined and plotted in Figs. 3 and 4 as a linear function of fission density.

The largest component of fuel swelling is due to the formation of fission gas bubbles. Turning first to the U_3Si_2 data in Fig. 3 it appears that this component is not linear with fission density at lower swelling values but tends to a linear behavior when swelling reaches higher levels. Also there appears to be a pronounced effect of enrichment as evidenced by the difference in swelling behavior of LEU, MEU, and HEU fuel. Although the higher enriched fuel swells much faster (with respect to time at power) its swelling rate with respect to fission density is clearly reduced. The non-linear behavior is caused by the capability of smaller bubbles to contain more gas atoms (have higher gas pressure) according to the following equilibrium equation

$$(P + \sigma + \frac{2\gamma}{r})\, V = nkT \qquad (1)$$

where P is the gas pressure in the bubble, σ the pressure restraining bubble growth due to the creep strength of the fuel and surrounding aluminum, and γ is the surface tension of the fuel.

The magnitude of γ is not well known and is usually taken to be on the order of 500-1000 dynes cm^{-1}. Thus the restraining force due to the surface tension term $\frac{2\gamma}{r}$ is significant for small bubble radii. In addition the high pressure gas in very small bubbles does not exhibit ideal behavior.

Gas bubbles are indeed small in U_3Si_2 at low fission densities as shown in Fig. 5. Up to a fission density of 3 x 10^{27} m^{-3} the bubbles are apparently below the resolution limit of the SEM (approximately 500Å) and fuel contains only isolated small patches or strings of bubbles that are associated with grain boundaries or second phases. The fuel surrounding these bubbles incidentally always contains some aluminum.

At a fission density of approximately 4 x 10^{27} m^{-3} a dense, relatively ordered, population of bubbles is present throughout the fuel. The bubble diameter increases at higher fission densities and the bubbles remain evenly distributed without any evidence of linking up even at full burnup of the LEU fuel.

The persistently regular spacing and uniform size of the bubbles in U_3Si_2 is very significant, for it explains the excellent swelling behavior of this fuel. This stable bubble morphology has been observed up to nearly 80% swelling in HEU fuel at a burnup of over 60% as shown in Fig. 6. In order to develop such a relatively ordered distribution and uniform size, the bubbles must nucleate rather simultaneously on a non-random "lattice" of nucleation sites. The range of gas diffusion to the bubbles must be limited to prevent the growth of certain bubbles at the expense of others and linkup of bubbles. We propose that the nucleation occurs on a cell structure of most likely polygonized, fission generated, dislocations. However, no experimental proof can be offered at this time.

Computer calculations utilizing state of the art models for fission gas behavior have shown that the bubble size distribution is bimodal; i.e., in addition to the larger visible bubbles that developed on dislocations, there is a population of much smaller bubbles in the matrix. These bubbles are not resolved by SEM in the LEU fuel but become partially visible at the higher fission densities achievable in MEU and HEU fuel as shown in Fig. 7.

The apparent fission rate dependence is due to a delay in development of larger (visible) bubbles when fission rate increases. As shown in Fig. 9, LEU fuel has developed the characteristic bubble morphology at a fission density of 4.2 x 10^{27} m^{-3} and has swollen to about 20%, while MEU fuel has not developed visible bubbles, has swollen only 12% and appears to have a microstructure similar to LEU fuel at a much lower fission density.

Intuitively one would argue that higher fission rate should have the opposite effect because higher fission rates result in higher fission induced defect production and diffusion, hence higher growth rates. The effect must therefore occur in the early nucleation and growth stage. Possible mechanisms being explored include the following.

It has been shown that higher radiation damage rate increases the recombination of radiation induced interstitials and vacancies, thereby decreasing the production of dislocation loops. It may be that the development of the aforementioned polygonized network of dislocations on which the eventually larger bubbles nucleate and grow is delayed at higher fisson rates. The problem with this is that dislocation networks in irradiated materials are usually established at relatively low doses and the dose rate effect needs therefore be very powerfull to fit the observed dose range at which U_3Si_2 swelling rate is lowered.

An alternate explanation could be due to the effect of certain fission product elements on the diffusion of vacancies and or fission gas. The concentration of certain medium-long halflife fission products is a function of fission rate. If these concentrations are high enough and if the elements have a large binding energy with vacancies a significant reduction in diffusivities is possible.

The most likely explanation, however, is that at higher fission rates a larger number of small matrix bubbles is formed and a larger amount of gas is maintained in a dynamic, fission induced, solution in the matrix. This gas, residing in the small matrix bubbles and in solution, is not available for growth of bubbles on dislocation. A higher absolute gas concentration, i.e., higher fission density is needed to start significant growth of the dislocation bubbles. This explanation has a problem as well, in that current bubble nucleation and growth models do not predict the magnitude of the observed effect.

Finally there may be an effect due to the difference in deformation rate of the aluminum surrounding the fuel particles. The creep strength of the aluminum provides an external restraint on bubble growth, particularly on larger bubbles where the surface tension is smaller (see Eq. 1). The aluminum creep rate is determined by the fast neutron flux at the present low temperatures. In as much as the flux is the same for all enrichments the radiation enhanced creep rate is so as well. Because of the higher swelling rate of HEU fuel, as a function of time at power, a higher stress in the aluminum is calculated compared to LEU fuel because the time required to relax these stresses is determined by the flux whereas the swelling of the fuel is determined by the fission rate, i.e., flux and enrichment.

It may be possible to glean more information from the large number of LEU plates, some of which were irradiated at significantly different flux positions in the reactor. However, this will require substantially more work.

It appears that the amount of fuel in the dispersion fuel (loading) has little effect on swelling within an enrichment group as evidenced by the similarity in behavior of LEU fuel over a range of 33 to 50 Vol.% fuel loadings, see Fig. 3. We may conclude that the restraining force afforded by the aluminum matrix and cladding does not depend strongly on the amount of aluminum present in the present fuel plate design.

It may be that all of the above mechanisms, or indeed entirely different ones, operate. This detailed remodeling of the swelling in U_3Si_2 obviously needs further work.

The swelling due to fission gas in U_3Si is quite different compared to U_3Si_2 as shown in Fig. 4. The swelling rate is not only higher initially but an extremely high swelling rate that results in fuel plate pillowing ensues at higher fission densities in all but the lowest loaded plates. The swelling in U_3Si is a direct result of the evolution of the bubble morphology. As shown in Fig. 10 the bubbles in U_3Si do not form in the uniform, relatively ordered, distribution seen in U_3Si_2 but vary widely in size and link up to form eventually very large cavities. One of the present authors has proposed that the high bubble growth rate is due to the fact that U_3Si becomes amorphous during irradiation [5]. Fissioning in the amorphous alloy enormously increases diffussion and decreases the plastic flow strength. At first glance there appears to be a fission rate effect on U_3Si swelling as well, however, the effect of fuel loading on swelling is much more pronounced and indeed masks any possible rate effect.

For example there is no clear difference for LEU and MEU highly loaded data and likewise for LEU and MEU medium loaded data. The high swelling rate (deformation rate) of this fuel makes it also very responsive to external restraints, i.e., to the aluminum surrounding the fuel particles. The rapid breakaway swelling leading to pillowing occurs when fuel particles touch and bubble interlink across several particles (see Fig. 10). This occurs at a lower swelling value (lower fission density) for high loadings. In the case of HEU which has only a nominally 14 Vol.% initial loading this interlinkage does not take place even at the maximum swelling shown in Fig. 4. In addition, at the more than 60 at.% burnup of the initial 93% ^{235}U, a large fraction of the original U_3Si has transformed to U_3Si_2 which is as we have seen very stable. The combination of low loading and lower swelling due to the transformation to U_3Si_2 and larger mechanical restraint, as argued for the HEU U_3Si_2 fuel, explains the absence of breakaway swelling in the HEU fuel plates.

IV. Conclusion

More accurate fuel swelling data can be obtained by determining the residual as-fabricated porosity in the fuel cores as a function of fission density. Analysis of these more accurate swelling data reveals an effect of fission rate on the development of the fission gas bubble morphology. Current models for fission gas behavior do not adequately explain the observed swelling data. Further detailed analysis and reexamination of models is necessary.

Acknowledgements

The authors should like to thank Messrs. J. L. Snelgrove, J. Rest and R. Birtcher for their helpful comments.

References

1. G. L. Hofman and L. A. Neimark, International Meeting on Reduced Enrichment for Research and Test Reactors, Nov. (1986), Gatlinburg, Tennessee, USA.
2. G. L. Hofman et al., International Meeting on Reduced Enrichment for Research and Test Reactors, Nov. (1985), Buenos Aires, Argentina.
3. G. L. Hofman, International Meeting on Reduced Enrichment for Research and Test Reactors, Oct. (1988), San Diego, California, USA.
4. J. Rest et al., Proc. Int. Symp. on Effects of Radiation on Materials, June (1988), Andover, Massachusetts, USA.
5. G. L. Hofman, Journal of Nucl. Mat. 140 (1986), pp 256-263.

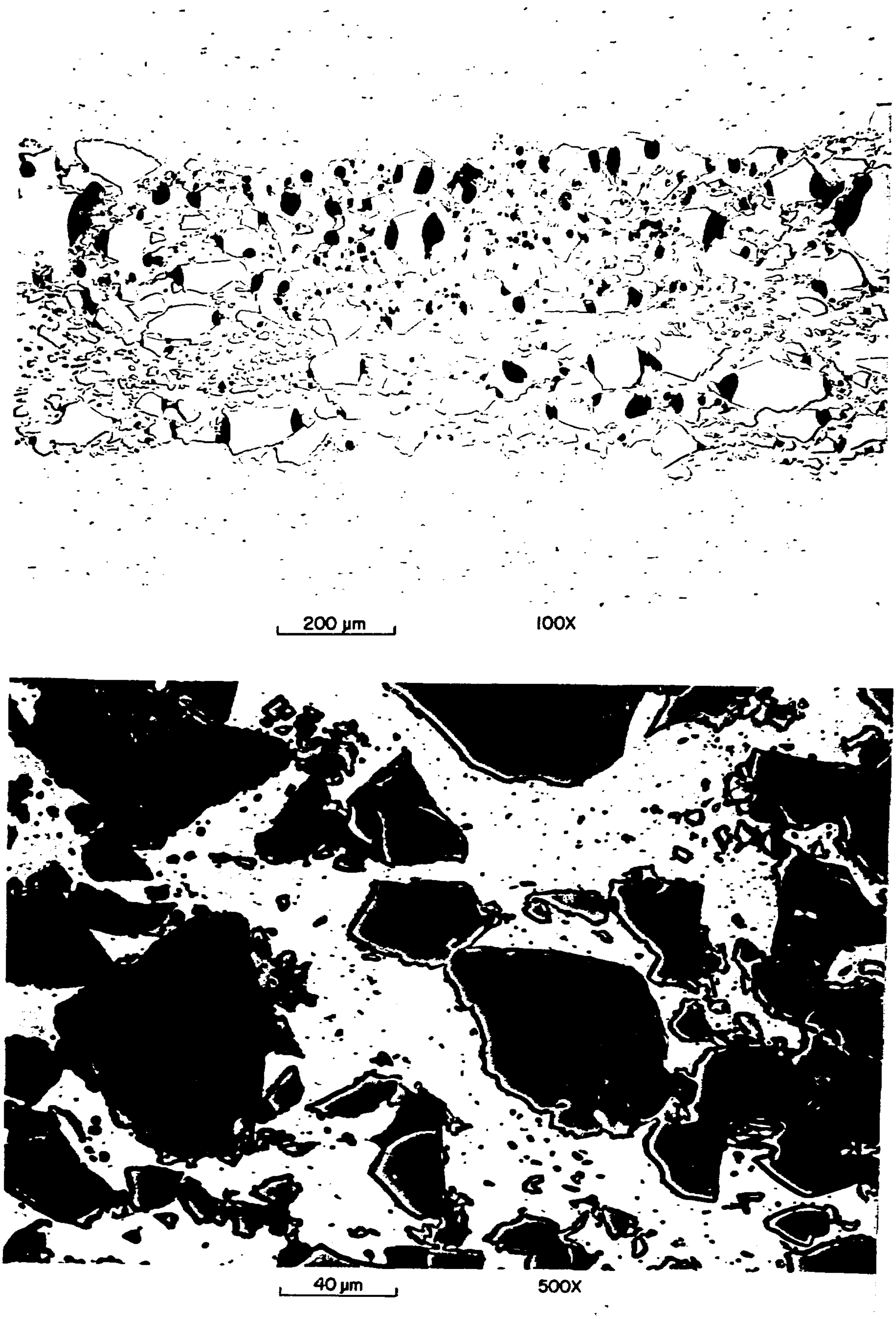

Fig. 1. As-fabricated porosity in depleted U_3Si_2 dispersion fuel after irradiation.

Fig. 2. REDUCTION OF AS-FABRICATED POROSITY AS A FUNCTION OF FISSION DENSITY IN THE FUEL IN U_3Si AND U_3Si_2

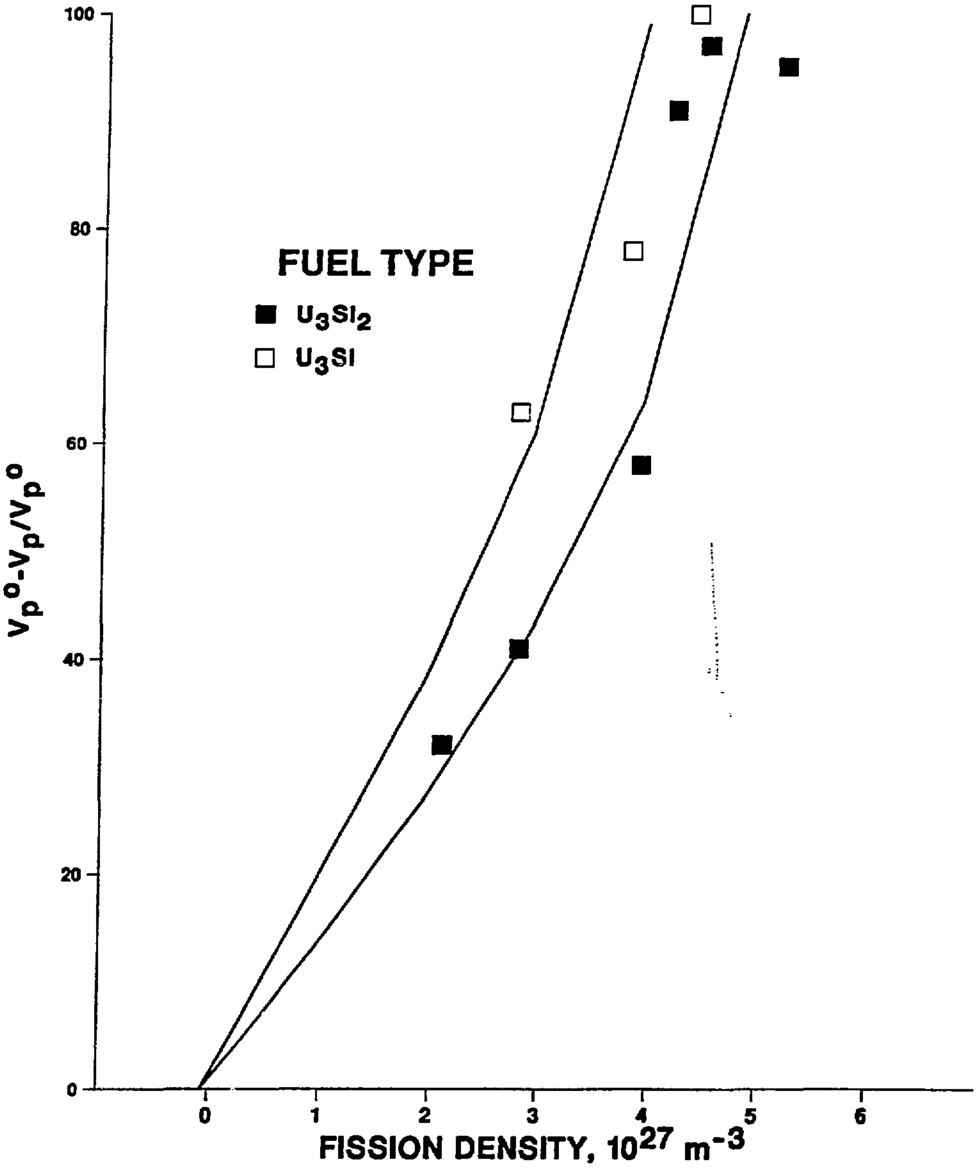

Fig. 3. FUEL SWELLING IN U_3Si_2 FOR VARIOUS ^{235}U ENRICHMENTS AND INITIAL FUEL VOLUME FRACTIONS (%) AS A FUNCTION OF FISSION DENSITY

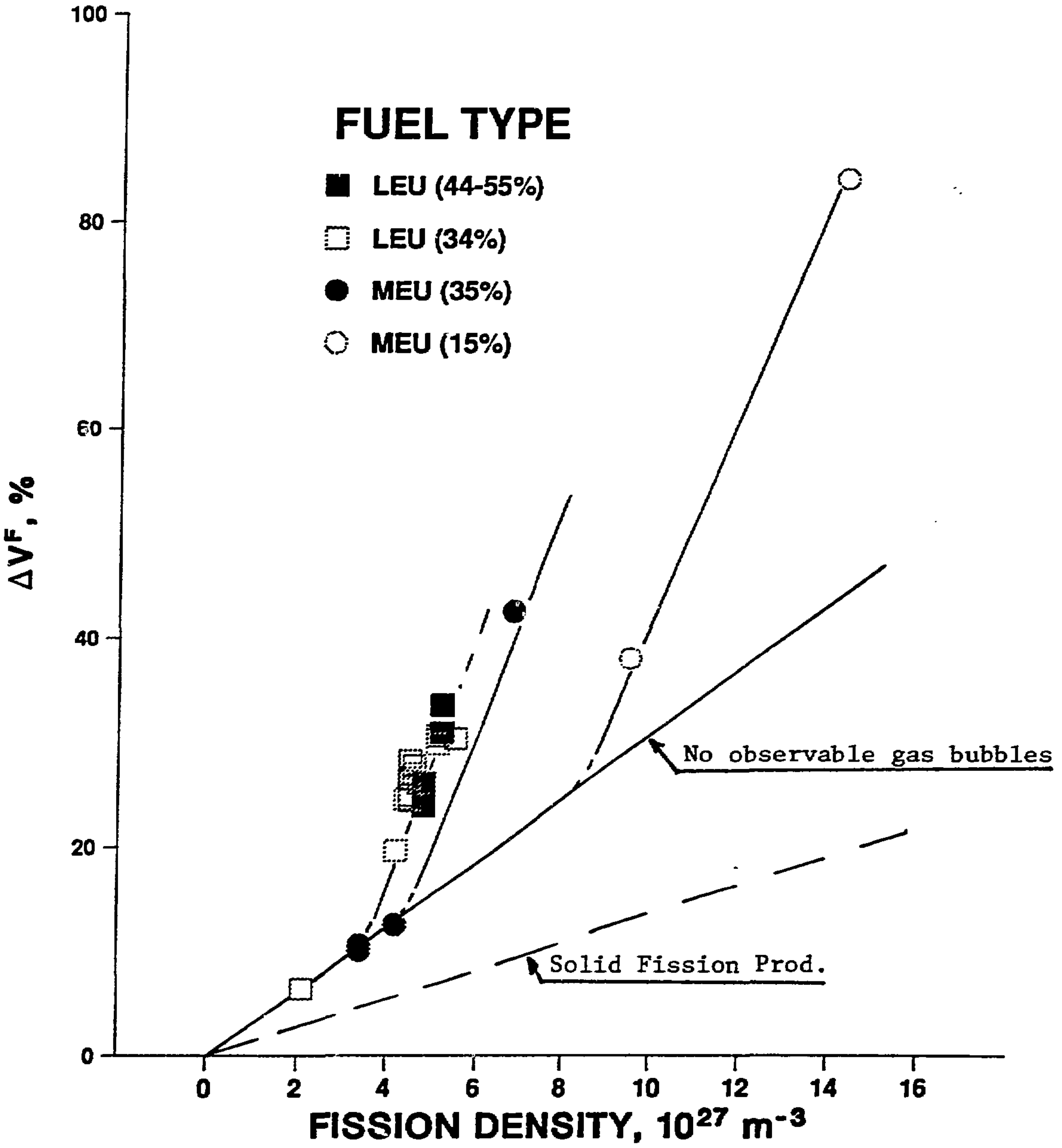

Fig. 4. FUEL SWELLING IN U_3SI FOR VARIOUS ^{235}U ENRICHMENTS AND INITIAL FUEL VOLUME FRACTIONS (%) AS A FUNCTION OF FISSION DENSITY

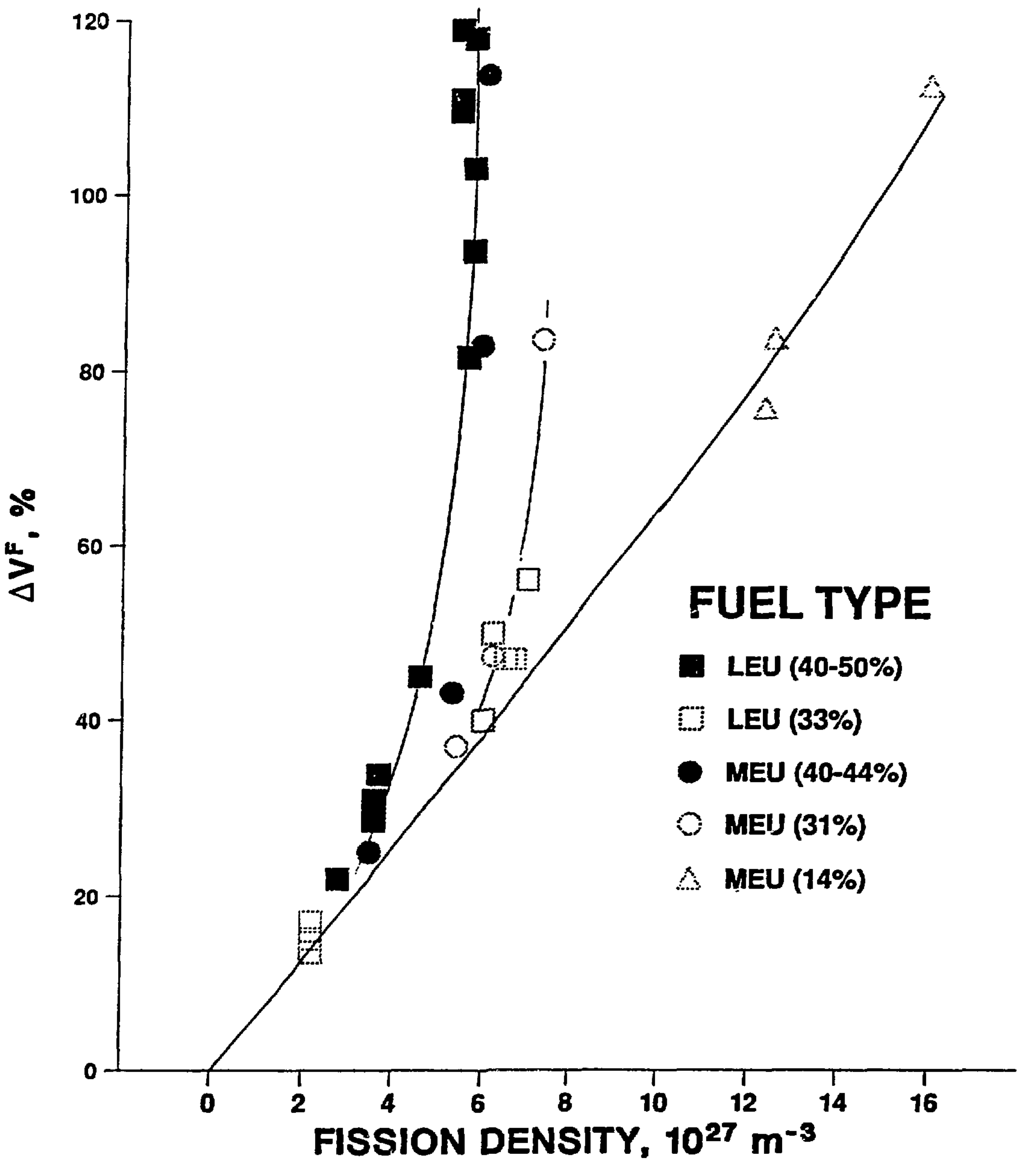

2.1×10^{27} cm^{-3}

3×10^{27} cm^{-3}

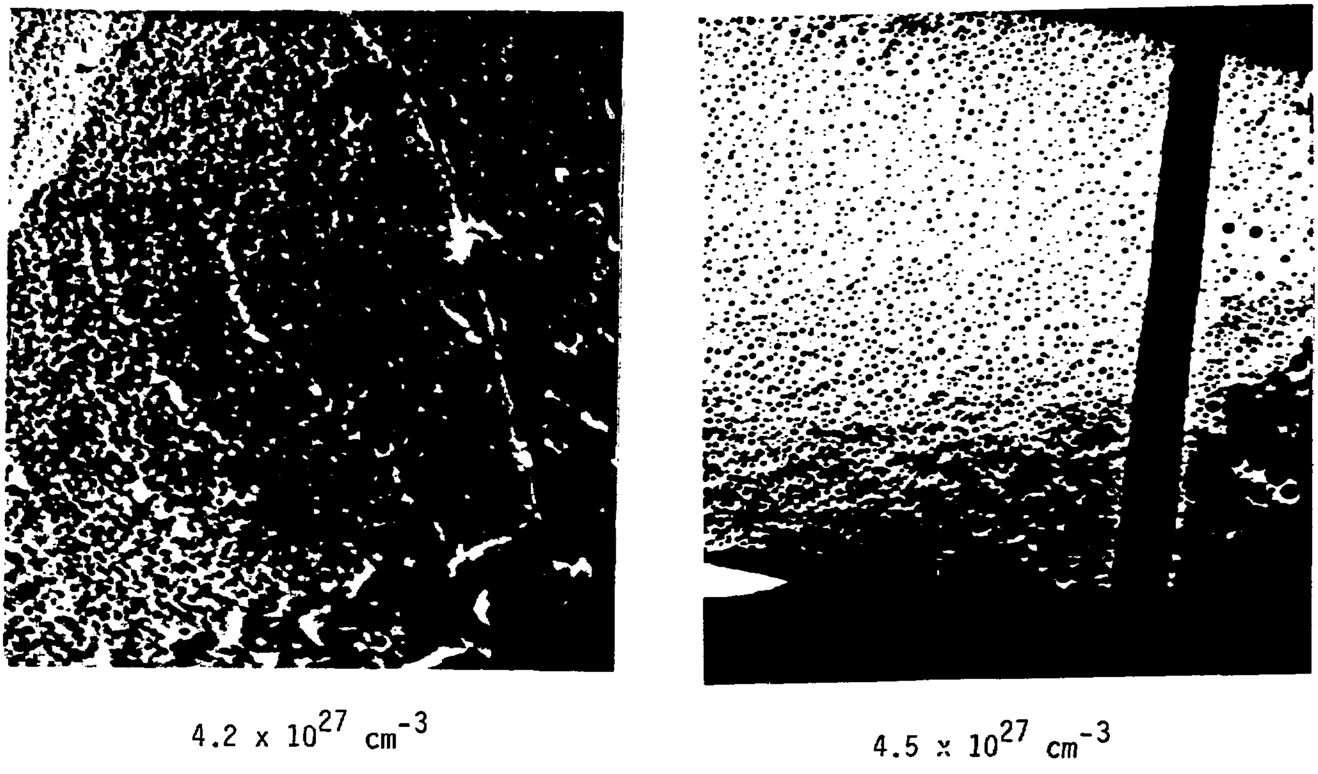

4.2×10^{27} cm^{-3}

4.5×10^{27} cm^{-3}

Fig. 5. Development of fission gas bubbles in LEU U_3Si_2 shown at 4 different fission densities.

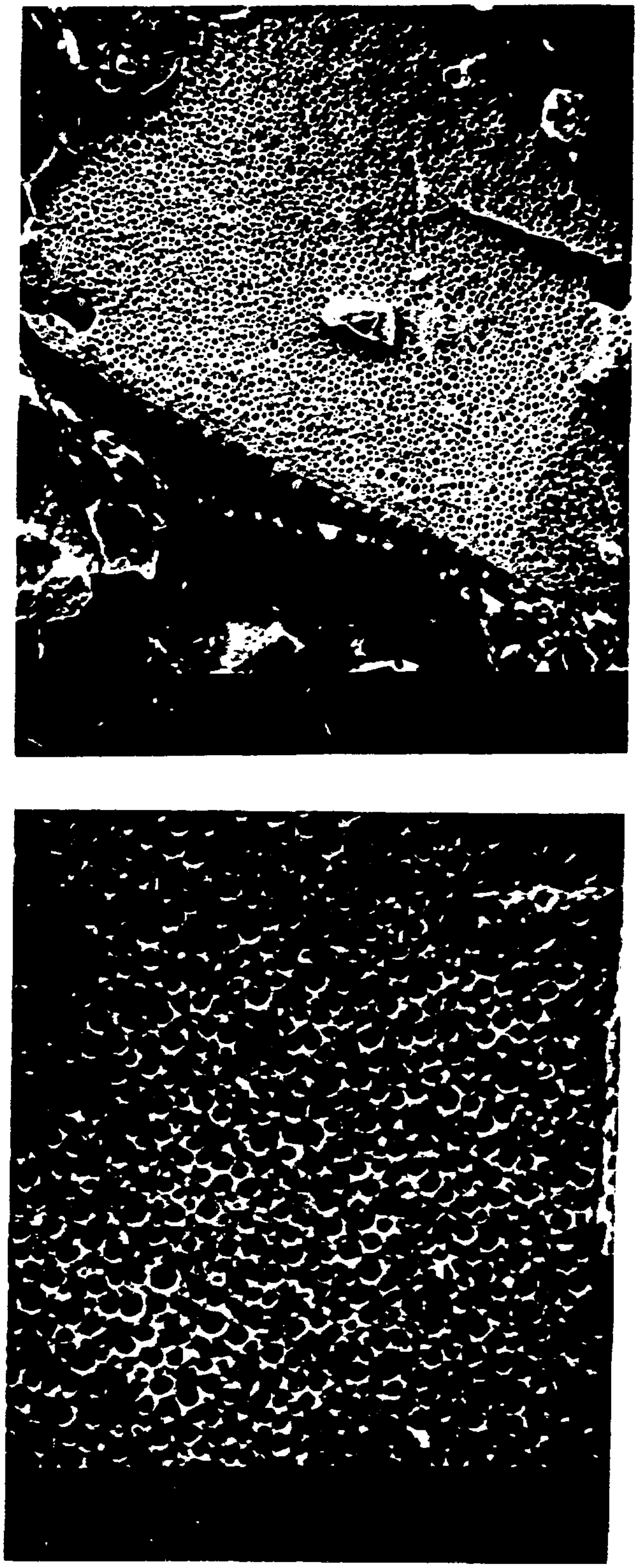

Fig. 6. Fission gas bubble morphology in HEU, U_3Si_2 at more than 60% ^{235}U burnup.

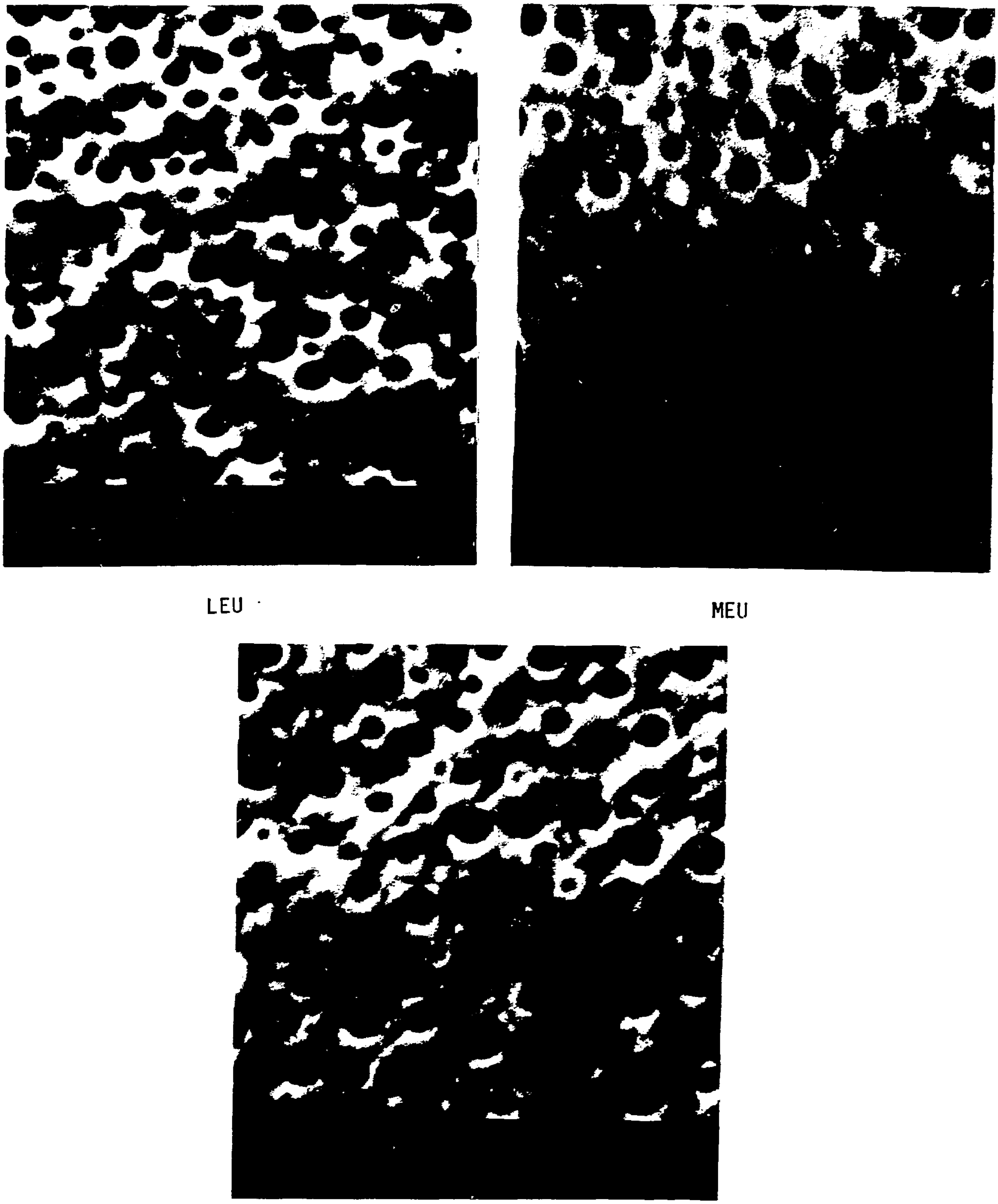

LEU

MEU

HEU

Fig. 7. Comparison of fission gas bubble distributions in LEU, MEU and HEU, U_3Si_2 at similar volume increase.

Fig. 8. AVERAGE FISSION GAS BUBBLE DIAMETER AS A FUNCTION OF FISSION DENSITY IN LEU, MEU, AND HEU -- U_3Si_2

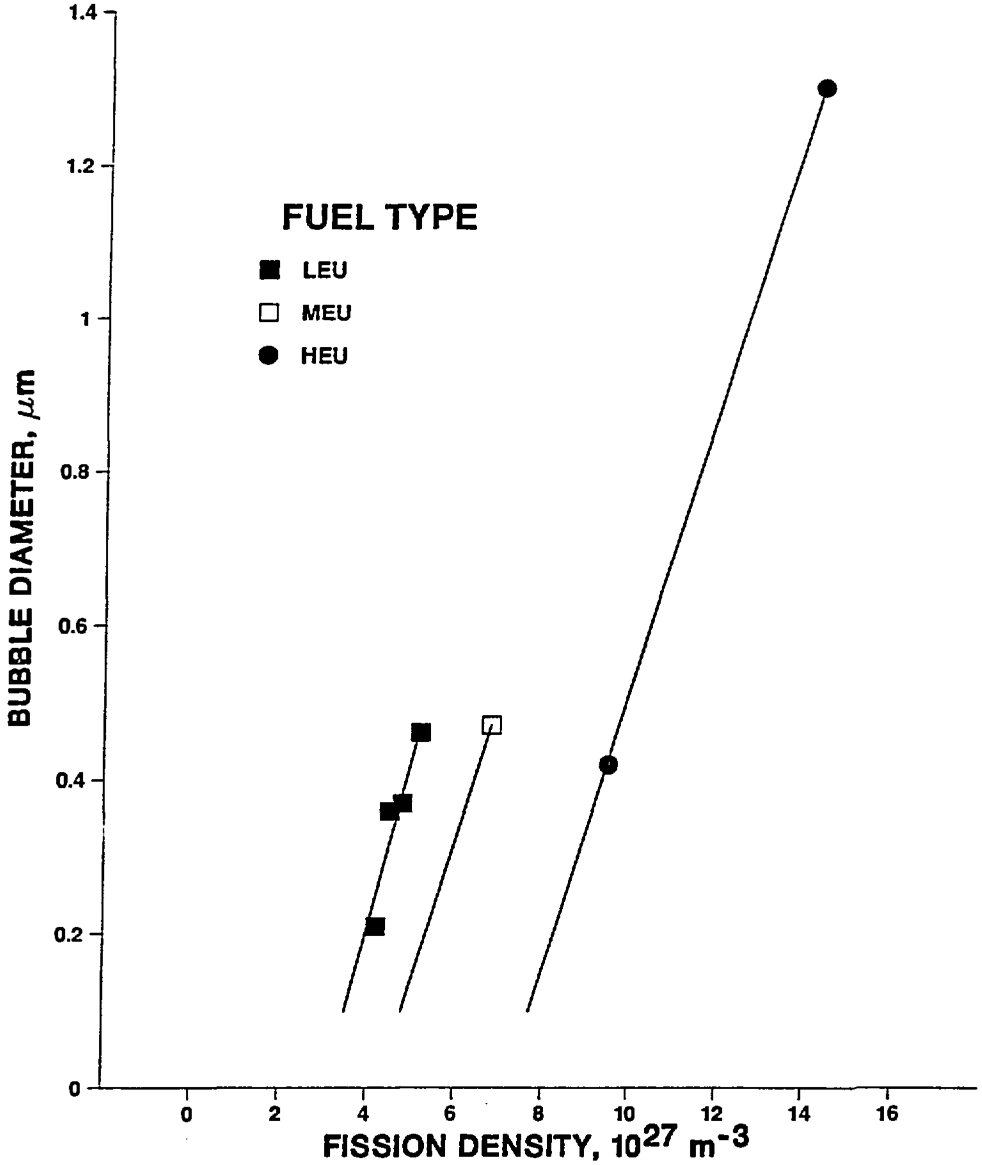

Fig. 8. AVERAGE FISSION GAS BUBBLE DIAMETER AS A FUNCTION OF FISSION DENSITY IN LEU, MEU, AND HEU -- U_3Si_2

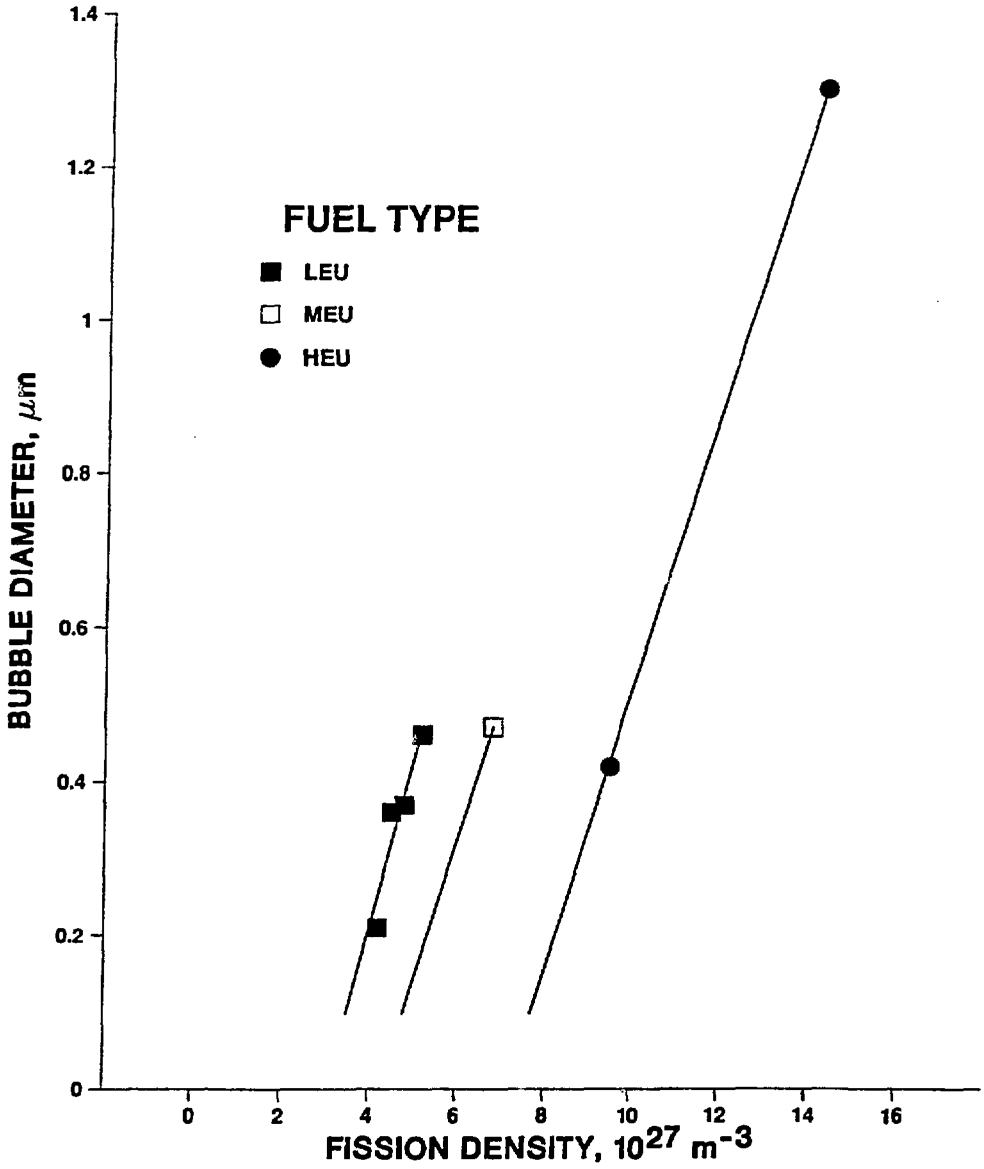

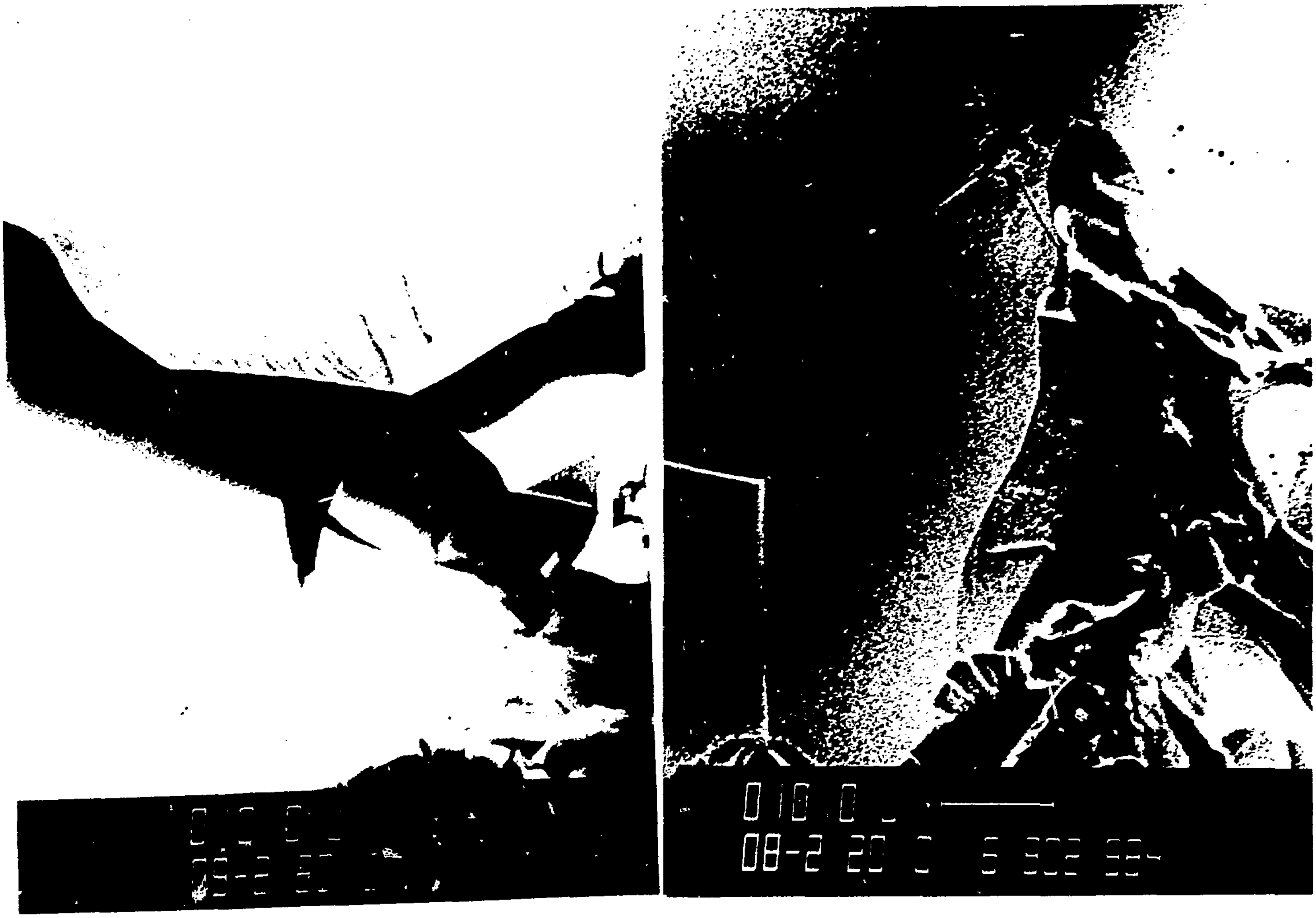

LEU, $2.1 \times 10^{27}\ \cancel{c}\mathrm{m}^{-3}$

MEU, $4.2 \times 10^{27}\ \cancel{c}\mathrm{m}^{-3}$

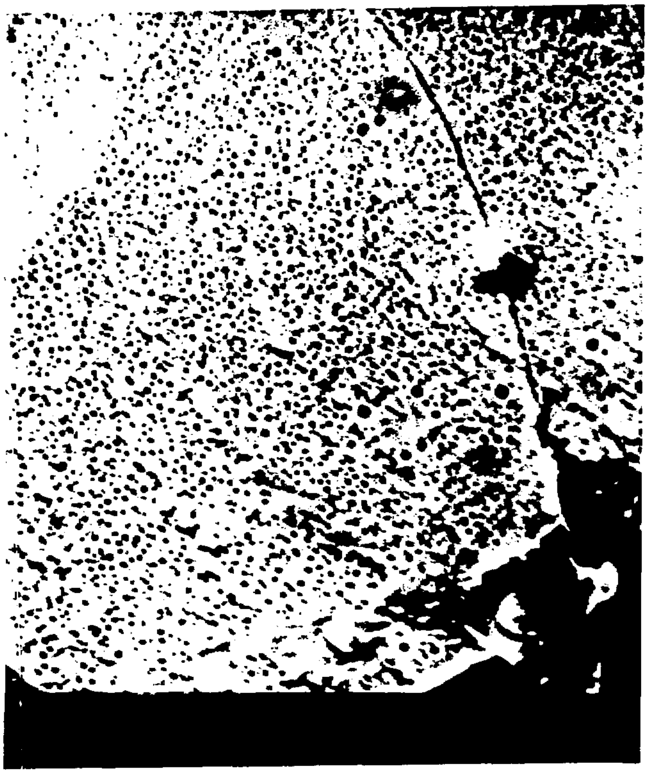

LEU, $4.2 \times 10^{27}\ \cancel{c}\mathrm{m}^{-3}$

Fig. 9. Difference in fission gas bubble development between LEU and MEU, U_3Si_2.

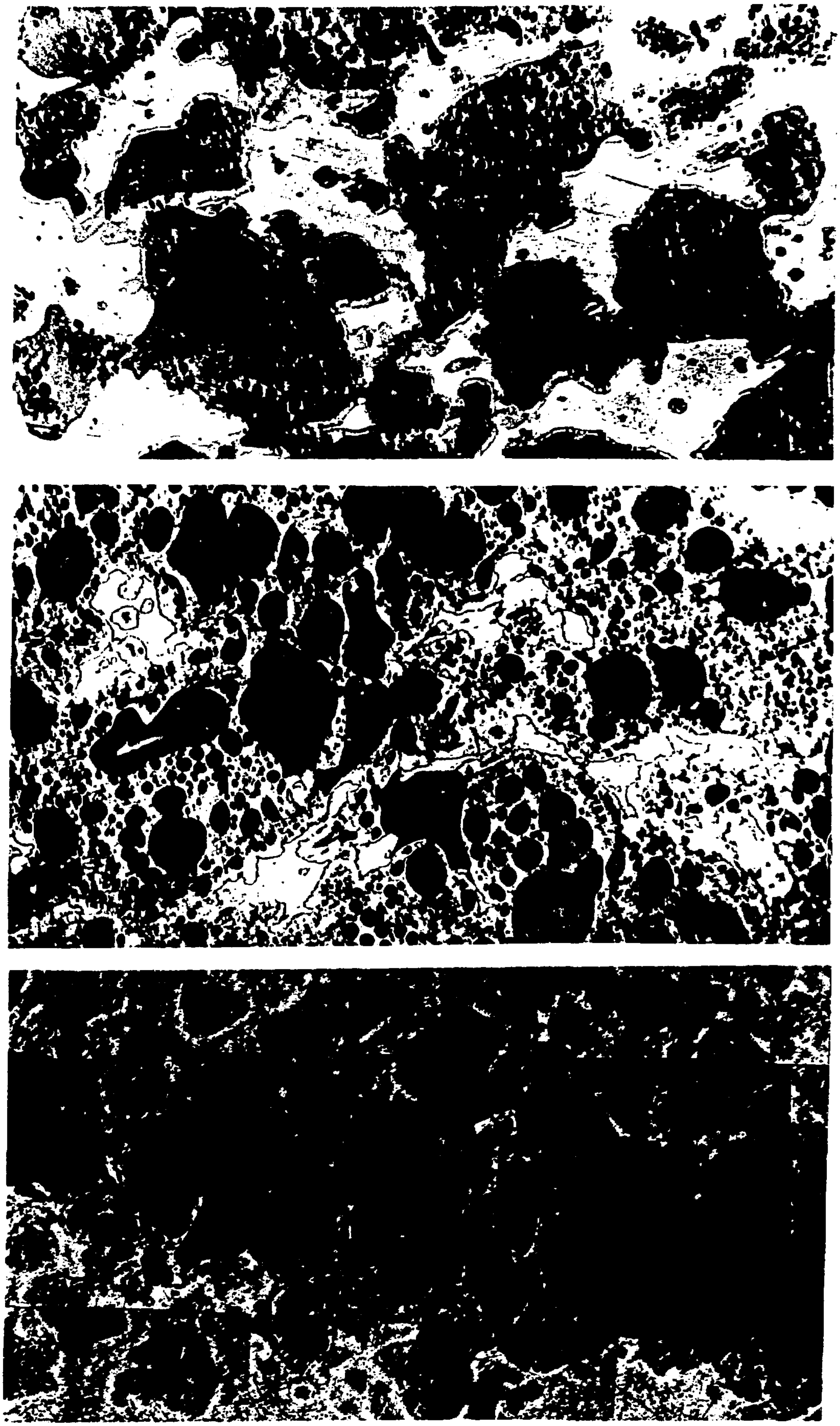

Fig. 10. Fission gas bubble development in LEU, U_3Si showing initial swelling stage, breakaway stage and pillowing.